ORGANIC CHEMISTRY FRONTIERS

RESEARCH ARTICLE

View Article Online
View Journal | View Issue

Cite this: *Org. Chem. Front.*, 2026, **13**, 3637

A co-registered molecular keypad lock for the generation of singlet oxygen

Jialei Chen-Wu, José A. González-Delgado and Uwe Pischel *

A dithienylethene (DTE)-anthracene dicarboximide dyad was prepared by condensation of an amino-substituted photoswitch with 2,3-anthracenedicarboxylic anhydride. The asymmetrically substituted dyad also includes a pyridine moiety, which provides a handle for further post-synthetic modifications (*e.g.*, the herein employed methylation). The methylated dyad can be photoswitched between the ring-open and ring-closed DTE forms in several cycles without noticeable fatigue, being the UV light-induced ring-closing much more efficient ($\Phi_{o\rightarrow c}$ = 0.11) than the ring-opening at >550 nm light irradiation ($\Phi_{c\rightarrow o}$ = 0.005). On the one hand, the ring-open form of the dyad shows significant blue fluorescence of the electronically-decoupled anthracene dicarboximide chromophore (λ_f = 427 nm, Φ_f = 0.19). However, this emission is quantitatively quenched by a highly efficient FRET process in the closed form of the dyad. On the other hand, the open form of the dyad also shows sufficient excited triplet-state population and subsequent sensitization of singlet-oxygen ($^1O_2$) formation (Φ_Δ = 0.21), which again is completely deactivated for the closed form of the DTE. The thus achieved dual light-control of $^1O_2$ formation can be interpreted as a molecular keypad lock and provides an interesting additional layer of functionality of $^1O_2$ photosensitizers (PSs). The concomitant observation of fluorescence enables the co-registered operation of the molecular device.

Received 9th March 2026,
Accepted 23rd April 2026

DOI: 10.1039/d6qo00295a

rsc.li/frontiers-organic

Introduction

The use of light to exert stimulus-controlled functions is particularly appealing due to its spatiotemporal character.[1] In this context photoswitches are especially valuable tools, enabling to toggle in a reversible manner between different states with contrasting structural and electronic properties.[2–5] This potential has been capitalized in a broad range of applications, including biological contexts, catalysis, information processing and storage, or materials science.[6–18]

One particular field of interest is the external control of the action of singlet-oxygen ($^1O_2$) photosensitizers (PSs), with potential benefits for a more selective mode of action.[19–24] When integrating photoswitches and PSs in molecular devices, it is possible to exert reversible ON/OFF sequences of $^1O_2$ generation.[25–30] This is based on the ability of one of the forms of the photoswitch to act as quencher of the excited singlet state of the PS, thereby inhibiting all follow-up processes. This includes the formation of excited triplet states by intersystem crossing (ISC) and in ultimate consequence energy transfer to triplet molecular oxygen ($^3O_2$), leading to the formation of $^1O_2$. In such setting, the formation of $^1O_2$ can be controlled in a double manner: by light of wavelength λ_1 that activates the photoswitch and another photonic stimulus at λ_2 that triggers the PS itself (see Fig. 1a).[26,31] The action of the photoswitch provides an additional layer of control and potentially enhances the spatially confined selectivity of $^1O_2$ formation, which may be of interest in photodynamic therapy, antibacterial treatments, or oxidative organic transformations.[28,32,33]

Among the various families of photoswitches that can be potentially employed for the outlined purposes are hemithioindigos, azobenzenes, spiropyrans, and dithienylethenes (DTEs).[26,28–30] Especially the latter stand out for their robust and all-photonic *modus operandi*. When combined with a PS, DTEs can modulate Förster resonance energy transfer (FRET) processes upon light irradiation,[34,35] providing a dynamic way to regulate $^1O_2$ formation. This was shown for intermolecular cocktail approaches, molecular dyads, and metal–organic frameworks that incorporate DTE and PS.[31–33,36–40] A large dynamic range of ON/OFF switching, meaning that practically only one of the photoswitch forms enables $^1O_2$ formation, is highly desirable. This requires a stringent molecular and photophysical design of the FRET process and the implicated energy donor–acceptor pair.

It is noteworthy that for many reported systems the control of $^1O_2$ production instead occurs partially, being generally

CIQSO – Center for Research in Sustainable Chemistry and Department of Chemistry, University of Huelva, Campus de El Carmen s/n, E-21071 Huelva, Spain. E-mail: uwe.pischel@diq.uhu.es

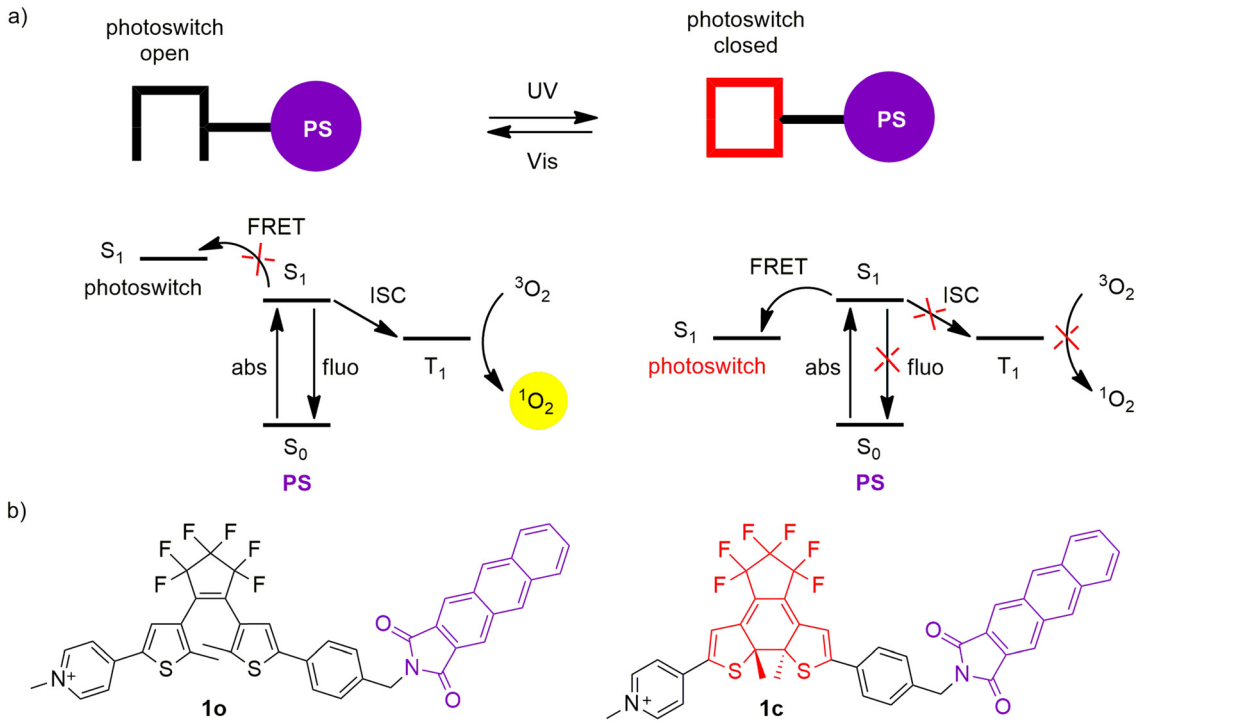

Fig. 1 Photochemical control of singlet oxygen formation and photoisomerization of **1**. (a) Schematic Jablonski diagrams demonstrating the interplay between excited state pathways in the different forms of the photoswitch. (b) Structures of the open (**1o**) and closed form (**1c**) of the herein investigated dyad.

described in qualitative terms. This limitation arises from the coexistence of multiple excited-state pathways, mainly FRET and photoinduced electron transfer (PeT), whose individual contributions are difficult to disentangle. As a result, establishing predictive relationships between molecular design and the associated photochemical performance remains a worthwhile objective. Herein we address this challenge by introducing a DTE-anthracene dicarboximide dyad (**1**, see Fig. 1b) that showcases clear-cut binary "all-or-nothing" switching of $^1O_2$ generation and the fluorescence of the PS. Although the parallel involvement of PeT is thermodynamically plausible, based on conservative estimates, the observed trend in $^1O_2$ formation consistently tracks FRET, providing a framework for the rational light-induced control of photosensitization.

Furthermore, the use of multiple light-input signals and the all-photonic switching of the DTE provide a means to implement the molecular design with the function of a keypad lock, where the order of application of the light inputs matters decisively for the binary value (*i.e.*, 0 or 1) of the functional output.[41–44] This usefully complements earlier works by the Akkaya group, who demonstrated the photosensitized formation of $^1O_2$ in dependence on AND logical operations with chemical and photonic inputs.[45–48] In addition, the dyad partitions the decay of the excited singlet state between radiative "fluorescent" deactivation and triplet state population *via* ISC.[49] This enables the co-registration of $^1O_2$ formation *via* the detection of fluorescence and establishes a "report-and-release" protocol.[50]

Results and discussion

Design and synthesis

The design of compound **1** is based on a perfluorinated DTE core due to its higher stability compared to fluorine-free analogues.[51] One arm of the DTE was functionalized with an anthracene dicarboximide unit, serving as the PS. Both functional units are connected through a benzyl spacer to ensure electronic decoupling. The other arm was substituted with a pyridine moiety to potentially allow the post-functionalization of the dyad, for instance by the S_N2 Menshutkin reaction with alkyl halides,[52] coordination with transition metals,[53] or *via* Zincke reactions for solid-phase synthesis of peptides,[54] thereby broadening its application spectrum. In this work, the straightforward methylation was chosen to demonstrate the ease of such modifications.

DTE **1** was prepared according to the synthetic route shown in Scheme 1. The central building block **DTE-I$_2$** was obtained by following a published procedure, starting from 2-methylthiophene.[55] Subsequent functionalization involved two sequential $Pd(PPh_3)_4$-catalyzed Suzuki coupling reactions. First, **DTE-I$_2$** was reacted with one equivalent of 4-pyridinylboronic acid, providing the mono-substituted **A1** in 30% yield. A second coupling reaction with one equivalent of 4-(aminomethyl)phenylboronic acid pinacol ester hydrochloride was performed in the presence of the XPhos ligand, affording the product **A2** in 45% yield. The free amine group of DTE **A2** was then condensed with 2,3-anthracenedicarboxylic anhydride.

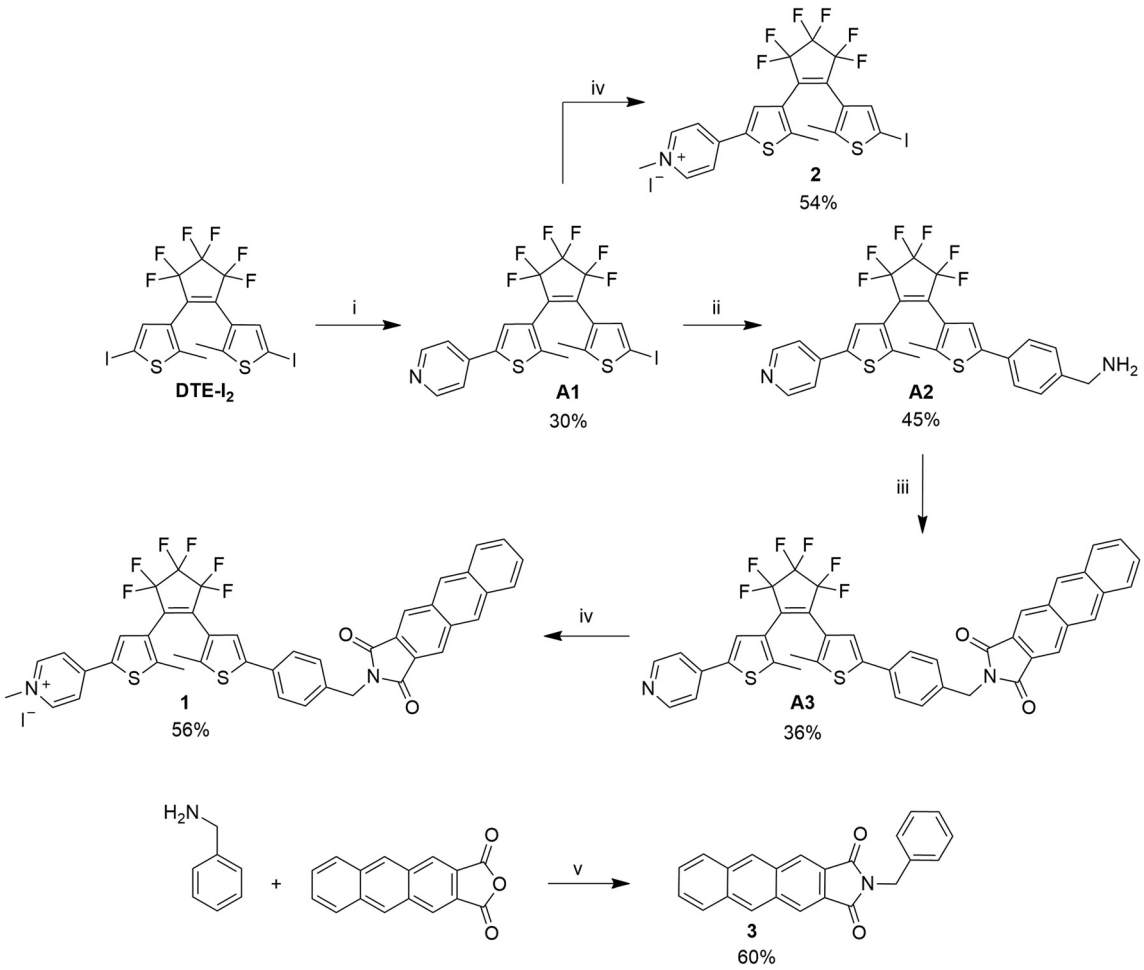

Scheme 1 Synthesis of **1**, **2**, and **3**. Reagents and conditions: (i) $Pd(PPh_3)_4$, Na_2CO_3, 4-pyridinylboronic acid, DME, H_2O, 90 °C. (ii) $Pd(PPh_3)_4$, Na_2CO_3, 4-(aminomethyl)phenylboronic acid pinacol ester hydrochloride, XPhos, DME, H_2O, 90 °C.; (iii) 2,3-anthracenedicarboxylic anhydride, EtOH, reflux; (iv) methyl iodide, DCM, rt; (v) EtOH, reflux. The chemical yield for each reaction is provided below the corresponding compound number in the scheme. All DTE-containing compounds were obtained in their open form and are shown like this.

The resulting compound **A3** was obtained in 36% yield. Finally, methylation of the pyridine moiety using methyl iodide afforded photoswitch **1** in 56% yield. For comparative studies, the model compound **2** was synthesized by direct methylation of **A1** with methyl iodide. Additionally, the anthracene dicarboximide **3** was prepared by condensation of 2,3-anthracenedicarboxylic anhydride with benzylamine and used as a model chromophore in this study. The new products were characterized by ^{1}H, ^{13}C, and ^{19}F NMR spectroscopy, gCOSY and gHSQC experiments, and high-resolution mass spectrometry (see SI).

Photochemistry

The most important photochemical and photophysical data of the herein investigated compounds are compiled in Table 1. The qualitative inspection of the UV/vis absorption spectra of the open and closed forms of **1** (*i.e.*, **1o** and **1c**, respectively) and the two model compounds **2** and **3** reveals the presence of both chromophores in dyad **1** (Fig. 2a). Furthermore, for **1o** the absorption spectrum corresponds to the sum of the spectra of the ring-open model DTE **2o** and **3** (Fig. 2a). This suggests that both chromophores are electronically decoupled by the benzyl bridge in the dyad, as was intended in the design approach. However, for **1c** there is a significant deviation of the long-wavelength absorption maximum in comparison to the ring-closed model DTE **2c**, which manifests in a difference of 37 nm. This is likely due to the acceptor$_1$–π–acceptor$_2$ character of **1c**, where the closed DTE core serves as π-bridge.

The colorless **1o** presents UV/vis absorption maxima at 350 and 403 nm. Upon irradiation at 365 nm (*ca.* 80% of the light is absorbed by the DTE core), a 6π electrocyclization reaction occurs, yielding the blue-colored **1c** with absorption maxima at 350, 405, and 653 nm (Fig. 3a). Furthermore, an isosbestic point at 375 nm was observed, suggesting a clean photochemical transformation without significant formation of secondary byproducts. The selective irradiation of **1c** with visible light (>550 nm) regenerates **1o** (Fig. 3b). Both photoswitching processes proceed with virtually quantitative transformation (100% pure isomer in the respective photostationary states), as

Table 1 Photophysical and photochemical properties of the compounds **1–3** in air-equilibrated acetone solutions

	λ_{abs} (nm) [ε(M^{-1} cm^{-1})]	$\Phi_{o\rightarrow c}$ [a]	$\Phi_{c\rightarrow o}$ [b]	λ_f (nm)	Φ_f [c]	τ_f (ns) [d]	Φ_Δ ($^1O_2$) [e]
1o	350 [29 900] 403 [7100]	0.11		427, 444	0.19	3.23 (89%) 6.00 (11%)	0.21
1c	350 [20 500] 405 [18 500] 653 [18 300]		0.005		[f]		[g]
2o	348 [27 600]	0.70					
2c	385 [10 500] [h] 616 [14 800] [h]		0.011				
3	381 [5800] 403 [6600]			431, 454	0.35	7.17 (100%)	0.58

[a] Determined by actinometry with potassium trioxalatoferrate(III) trihydrate ($K_3Fe(C_2O_4)_3 \times 3\ H_2O$); 20% error; ref. 56 and 57. [b] Determined by actinometry with 1,2-bis(2,4-dimethyl-5-phenyl-3-thienyl)-3,3,4,4,5,5-hexafluoro-1-cyclopentene; 20% error; ref. 58 and 59. [c] Fluorescence quantum yield (excitation of the anthracene dicarboximide chromophore at 403 nm), determined with an integrating sphere; 10% error. [d] Fluorescence lifetime, measured by time-correlated single-photon-counting; 5% error. In parentheses the relative weight of each lifetime component is given, when multi-exponential decay was observed. [e] Efficiency of $^1O_2$ formation (25% error) determined with Rose Bengal as standard; ref. 60. [f] The minor fluorescence that is detected for **1c** is ascribed to a residual amount of **1o** in the photostationary state. [g] No formation of $^1O_2$ was observed. [h] The molar absorption coefficient ε for the closed form **2c** is corrected for the presence of a minor amount of **2o** (4%) in the photostationary state.

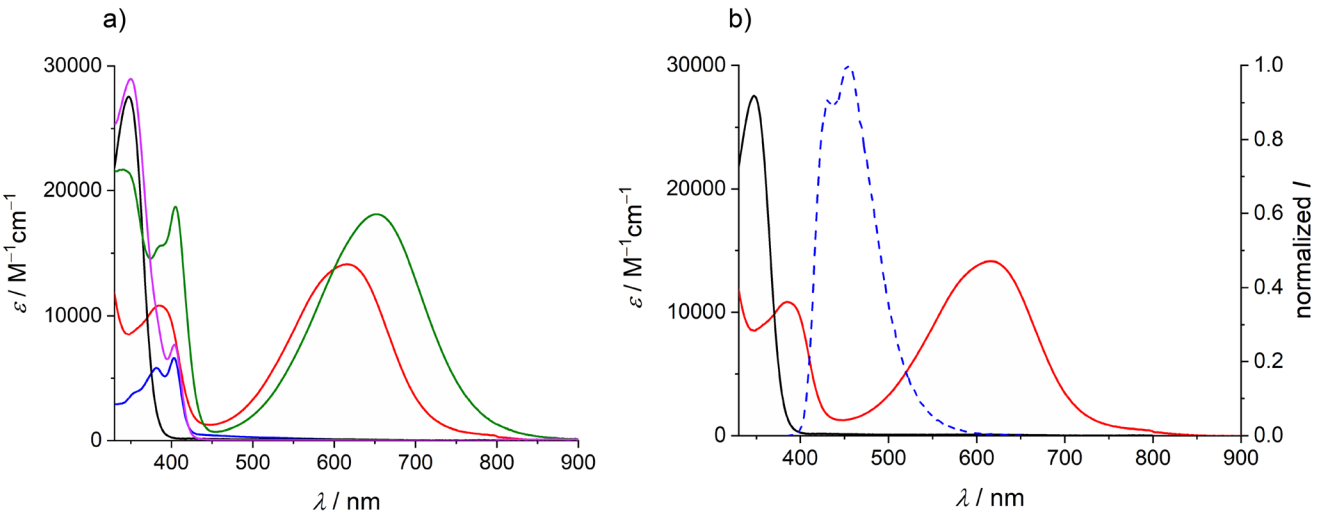

Fig. 2 (a) UV/vis absorption spectra of **1o** (magenta), **1c** (green), **2o** (black), **2c** (red), and **3** (blue) in acetone (all at 10 μM). (b) UV/vis absorption spectra of **2o** (black), **2c** (red), and emission spectrum of **3** (blue dashed line) in acetone. These spectra are shown separately for a better appreciation of the spectral overlap between the anthracene dicarboximide emission and the UV/vis absorption of the DTE core for **2c**, but not for **2o**. This clear-cut differentiation of spectral overlap leads to the observed "all or nothing" FRET process in dependence on the isomerization state of the DTE.

determined by ^1H NMR spectroscopy (see the SI). DTE **1** can be switched multiple times by alternating UV- and visible-light irradiation, exhibiting high fatigue resistance (Fig. 3d).

The photocyclization quantum yield ($\Phi_{o\rightarrow c}$) of **1o** at 365 nm excitation was determined using the ferrioxalate actinometer,[56,57] yielding a value of 0.11. The cycloreversion quantum yield ($\Phi_{c\rightarrow o}$) for irradiation at 580 nm is much smaller, with a value of 0.005, as determined with the DTE derivative 1,2-bis(2,4-dimethyl-5-phenyl-3-thienyl)-3,3,4,4,5,5-hexafluoro-1-cyclopentene.[58,59] It is noteworthy that compared with the model DTE **2o** ($\Phi_{o\rightarrow c}$ = 0.70), the photocyclization quantum yield is much lower for **1o**. We assign this tentatively to the occurrence of competing excited-state processes of the DTE moiety in **1o**, such as PeT involving the strongly electron-accepting anthracene dicarboximide or the methylpyridinium; see SI.[61] In line with this assumption is the observation that in the more polar acetonitrile $\Phi_{o\rightarrow c}$ drops even further to 0.07.

Fluorescence properties and energy transfer

The excitation of the anthracene dicarboximide chromophore produces an intense blue emission with two maxima at 427 and 444 nm (see Fig. 3c) and an emission quantum yield of Φ_f = 0.19 (see Table 1 for all fluorescence properties). Due to the electronic decoupling between both chromophoric moieties, the emission of **1o** originates exclusively from the anthracene dicarboximide. The corresponding excitation spectrum, monitoring the blue emission, shows solely the features of the anthracene dicarboximide chromophore, including its typical

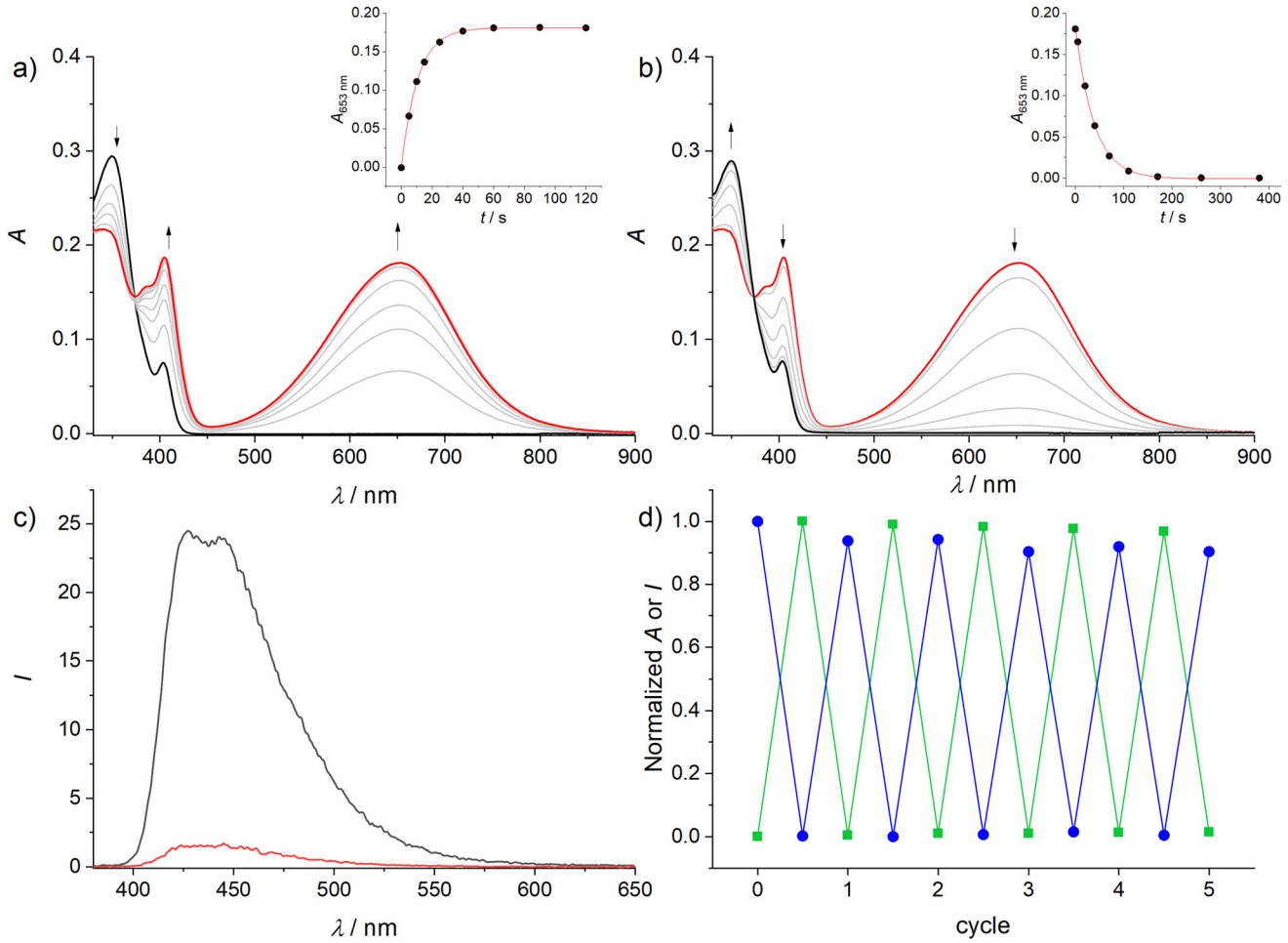

Fig. 3 UV/vis absorption spectra (top) and corresponding kinetic plots (insets) of DTE **1** (10 μM) in acetone. (a) ring closure by irradiation at 365 nm, (b) ring opening by irradiation at >550 nm; (c) emission spectra for excitation at 375 nm (black **1o**, red **1c**); (d) vis absorption (at 653 nm) and emission (at 444 nm) in repeated switching cycles (green – vis absorption, blue – emission).

fine structure. In addition, the model anthracene dicarboximide **3** yields quite identical fluorescence emission (Table 1 and Fig. 2b) and excitation spectra. Interestingly, the fluorescence quantum yield of **3** (Φ_f = 0.35) is nearly twice the value of the one observed for **1o**. The trend of the quantum yields is paralleled by the fluorescence lifetimes [3.23 ns for **1o** *versus* 7.17 ns for **3**], pointing to very comparable radiative rate constants of the individual fluorophore **3** and when integrated in the dyad **1o**. Hence, the inherent radiative properties are conserved in **1o** and differences in fluorescence relate to the occurrence of additional non-radiative deactivation (*e.g.*, PeT) in the dyad.

As noted for the reduced photocyclization quantum yield of **1o** (see above), the observed fluorescence quenching [comparing **1o** and **3**; $Q = (1 - \Phi_f(\mathbf{1o})/\Phi_f(\mathbf{3})) \times 100\%$] hints on the occurrence of competing intramolecular excited state pathways, *i.e.*, PeT from the DTE core to the excited singlet-state anthracene dicarboximide; see SI. As a matter of fact, while the fluorescence quenching Q amounts to 46% in acetone, it is further accentuated in the more polar solvent acetonitrile (Q = 60%).

The closed form **1c** shows further quenching and exhibits only very residual fluorescence, which moreover is attributed to a very minor content of **1o** in the photostationary state. In fact, the quantitative fluorescence quenching in **1c** is related to a highly efficient Förster resonance energy transfer (FRET) from the excited singlet anthracene dicarboximide to the ring-closed DTE core.[62] The occurrence of FRET in **1c** is experimentally substantiated by the fact that the fluorescence of the anthracene dicarboximide donor and the absorption of the ring-closed DTE acceptor overlap to a considerable degree ($J_{\text{dipole–dipole}} = 1.0 \times 10^{-11}$ cm^6 mol^{-1}). The calculation of the critical FRET radius R_0 (see SI), which is the donor–acceptor distance for which 50% FRET efficiency is expected, yielded a value of 41 Å. The actual donor–acceptor distance (R) was approximated by simple MM2 force-field modeling of the molecular structure of **1c**, yielding a value of about 14 Å. Based on these data the theoretically expected Φ_{FRET} amounts to practically 1, coinciding with the experimental observation of virtually quantitative fluorescence quenching. It is noteworthy that for **1o** no FRET quenching applies due to the absence of

absorbance of the DTE core (model **2o**) at wavelengths longer than 400 nm (Fig. 2b), yielding a zero spectral overlap with the anthracene dicarboximide fluorescence spectrum.

Generation of $^1O_2$

The fluorescence quantum yield of the anthracene dicarboximide moiety in **1o** points to the fact that a significant part (*ca.* 81%) of the excited singlet state decays non-radiatively. One quenching pathway is the abovementioned possibility of PeT. Akin to other anthracene derivatives, we infer the parallel involvement of the formation of excited triplet states *via* ISC. The excited triplet state may then be quenched by oxygen and lead to the energy-transfer sensitized formation of $^1O_2$. Indeed, upon excitation of **1o** at 419 nm, addressing selectivity the anthracene dicarboximide part, the typical near-infrared (NIR) phosphorescence of $^1O_2$ with a maximum at 1275 nm was detected (Fig. 4). This provides unambiguous evidence for the capacity of **1o** to act as PS. The overall quantum yield for $^1O_2$ formation was determined as Φ_Δ = 0.21. Performing the same experiment with the previously ring-closed dyad, that is, with **1c**, showed no sign of $^1O_2$ phosphorescence (Fig. 4). Upon visible-light irradiation, the system reverted to the open form **1o** with full recovery of $^1O_2$ generation capability. This process can be repeated without notable fatigue, as herein demonstrated for five cycles (inset of Fig. 4). The incapacity of **1c** to act as PS is reasoned with the quenching of the excited singlet state of the anthracene dicarboximide by FRET (see above),[62] which consequently disables the population of the excited triplet state and ultimately the observation of $^1O_2$ formation. The quantum yield for $^1O_2$ formation of **1o** is lower than that of model **3** (Φ_Δ = 0.58). Due to the plausible competition of PeT with the other S_1 deactivation channels (among them ISC and T_1 population) of the anthracene dicarboximide moiety in **1o**, less T_1 state is formed, which directly translates into reduced $^1O_2$ formation as compared to **3**.

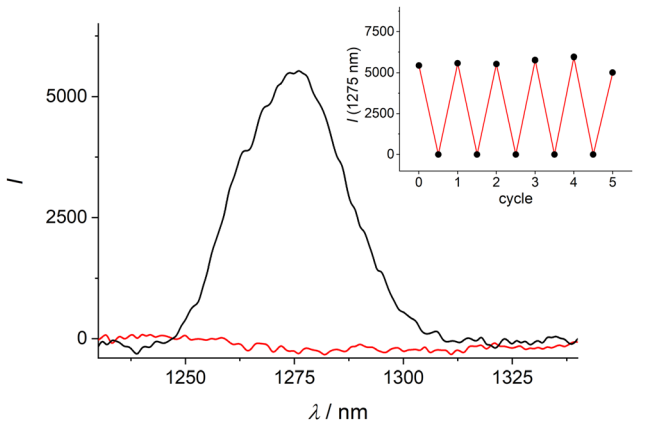

Fig. 4 $^1O_2$ phosphorescence spectra upon excitation of **1o** (black line) or **1c** (red line) at 419 nm; [**1**] = 10 μM. The inset shows the corresponding variations of emission intensity of singlet oxygen upon five photoswitching cycles, toggling between **1o** and **1c** by alternating irradiation at 365 nm and at >550 nm.

Table 2 Commented truth table for the all-photonic molecular keypad operation of **1c**

In_1 (>550 nm)	In_2 (419 nm)	Out_1 ($^1O_2$)	Out_2 (fluo)	Chemical observation
0	0	0	0	No photoprocesses
1	0	0	0	Only **1c** → **1o**
0	1[a]	0	0	Quenching of $^1O_2$ formation in **1c**
1 (2nd)	1 (1st)	0	0	Quenching of $^1O_2$ formation in **1c** and subsequent **1c** → **1o**
1 (1st)	1 (2nd)	1	1	First **1c** → **1o** and subsequent unquenched photosensitized $^1O_2$ formation by **1o**

[a] Although the excitation at 419 nm may also directly address the ring-closed DTE chromophore, the quantum yield of the ring opening is effectively too small to yield sufficient amounts of **1o**.

Molecular keypad lock

The photoswitching of **1** and the resulting modulation of its capability to photosensitize the formation of $^1O_2$ can be interpreted in the context of molecular logic operations.[42–44] Starting with the dyad in its closed form **1c** and choosing photonic signals as inputs In (In_1: irradiation at >550 nm; In_2: irradiation at 419 nm), the following Boolean logic can be realized (Table 2). No light irradiation (In_1 = In_2 = 0) leaves the dyad in the **1c** state and no $^1O_2$ formation is observed (Out_1 = 0). The irradiation at >550 nm (In_1 = 1) leads to ring opening (**1o**), but in the absence of the excitation of the anthracene dicarboximide (In_2 = 0) the output signal remains in the binary 0 state. Because of the described FRET, the same lack of $^1O_2$ formation is observed for the excitation of the anthracene dicarboximide (In_2 = 1) of **1c**, in the absence of irradiation at >550 nm (In_1 = 0). Only if both photonic input signals are activated (In_1 = In_2 = 1) $^1O_2$ could be in principle generated. However, this is only the case (Out_1 = 1) if the inputs are applied in the sequential order In_1 first (**1c** → **1o**) and then In_2. If this input order is reversed (In_2 before In_1) only the formation of **1o** results, but no $^1O_2$ is generated (Out_1 = 0). In addition, the same observations relate to the generation of fluorescence (see Table 2), which is only observed for **1o**. This constitutes a case of a co-registered logic gate operation.[50]

This overall logic behavior is coincident with a 2-input priority AND gate (2-PAND), a simple representation of a keypad lock.[44] It is noteworthy, that the input and output signals are all of photonic nature. In addition, the reversibility and high fatigue resistance of the photoswitching enable the recyclable operation of this molecular keypad lock. Furthermore, by application of 365 nm light the dyad can be conveniently reset to the initial state (**1o** → **1c**).

Conclusion

The meticulous photophysical design of the dithienylethene (DTE)-anthracene dicarboximide dyad **1** enabled the clear-cut and robust photoswitching of "all-or-nothing" $^1O_2$ formation.

This was enabled by the exclusive occurrence of FRET for the closed form of the photoswitch, while the open form showed zero spectral overlap between DTE absorption and anthracene dicarboximide PS emission. The dual light control of singlet-oxygen formation provides an additional layer of functionality to the action of PSs, potentially leading to increased selectivity. Further, it was shown that the dyad can be operated in a way so that a specific order of light inputs is required to observe singlet oxygen and fluorescence as outputs, akin to the function of a molecular co-registered 2-input priority AND gate or keypad lock.

Author contributions

J. C.-W.: investigation, formal analysis, validation, writing – original draft, writing – review & editing; J. A. G.-D.: investigation, writing – review & editing; U. P.: conceptualization, resources, funding acquisition, supervision, writing – review & editing.

Conflicts of interest

There are no conflicts to declare.

Data availability

The data supporting this article have been included as part of the supplementary information (SI). Supplementary information is available. See DOI: **https://doi.org/10.1039/d6qo00295a**.

Acknowledgements

This work was supported by the Spanish Ministry of Science, Innovation, and Universities (MCIU/AEI/10.13039/501100011033) and the European Regional Development Fund ERDF (grants PID2020-119992GB-I00 and PID2023-152556NB-I00). J. C.-W. was contracted through the EIC PATHFINDER project 101098934 – 4for2 (EISMEA – European Innovation Council and SMEs Executive Agency).

References

1 C. Brieke, F. Rohrbach, A. Gottschalk, G. Mayer and A. Heckel, Light–controlled tools, *Angew. Chem., Int. Ed.*, 2012, **51**, 8446–8476.
2 B. L. Feringa and W. R. Browne, *Molecular switches*, John Wiley & Sons, New York, USA, 2011.
3 A. Goulet-Hanssens, F. Eisenreich and S. Hecht, Enlightening materials with photoswitches, *Adv. Mater.*, 2020, **32**, 1905966.
4 M. M. Russew and S. Hecht, Photoswitches: from molecules to materials, *Adv. Mater.*, 2010, **22**, 3348–3360.
5 J. Volarić, W. Szymanski, N. A. Simeth and B. L. Feringa, Molecular photoswitches in aqueous environments, *Chem. Soc. Rev.*, 2021, **50**, 12377–12449.
6 Y. Yokoyama, Fulgides for memories and switches, *Chem. Rev.*, 2000, **100**, 1717–1740.
7 H. D. Bandara and S. C. Burdette, Photoisomerization in different classes of azobenzene, *Chem. Soc. Rev.*, 2012, **41**, 1809–1825.
8 M. Irie, T. Fukaminato, K. Matsuda and S. Kobatake, Photochromism of diarylethene molecules and crystals: memories, switches, and actuators, *Chem. Rev.*, 2014, **114**, 12174–12277.
9 R. Klajn, Spiropyran-based dynamic materials, *Chem. Soc. Rev.*, 2014, **43**, 148–184.
10 M. M. Lerch, S. J. Wezenberg, W. Szymanski and B. L. Feringa, Unraveling the photoswitching mechanism in donor–acceptor Stenhouse adducts, *J. Am. Chem. Soc.*, 2016, **138**, 6344–6347.
11 C. Petermayer and H. Dube, Indigoid photoswitches: visible light responsive molecular tools, *Acc. Chem. Res.*, 2018, **51**, 1153–1163.
12 F. G. Blandón-Cumbreras, M. Villabona, J. Osmólska, E. F. Petrusevich, D. B. Guzmán Ríos, R. Zaleśny, J. Olesiak-Bańska, J. Hernando and U. Pischel, Photoswitching of the two-photon absorption of donor-acceptor substituted dithienylethenes, *ChemistryEurope*, 2025, **3**, e202500072.
13 M. Villabona, S. Wiedbrauk, F. Feist, G. Guirado, J. Hernando and C. Barner-Kowollik, Dual-wavelength gated oxo-diels-alder photoligation, *Org. Lett.*, 2021, **23**, 2405–2410.
14 G. Cabré, A. Garrido-Charles, M. Moreno, M. Bosch, M. Porta-de-la-Riva, M. Krieg, M. Gascón-Moya, N. Camarero, R. Gelabert and J. M. Lluch, Rationally designed azobenzene photoswitches for efficient two-photon neuronal excitation, *Nat. Commun.*, 2019, **10**, 907.
15 R. Castagna, G. Maleeva, D. Pirovano, C. Matera and P. Gorostiza, Donor–acceptor stenhouse adduct displaying reversible photoswitching in water and neuronal activity, *J. Am. Chem. Soc.*, 2022, **144**, 15595–15602.
16 Z. Wang, H. Hölzel and K. Moth-Poulsen, Status and challenges for molecular solar thermal energy storage system based devices, *Chem. Soc. Rev.*, 2022, **51**, 7313–7326.
17 E. Siemes, O. Nevskyi, D. Sysoiev, S. K. Turnhoff, A. Oppermann, T. Huhn, W. Richtering and D. Wöll, Nanoscopic visualization of cross–linking density in polymer networks with diarylethene photoswitches, *Angew. Chem., Int. Ed.*, 2018, **57**, 12280–12284.
18 F. Li, M. Li, Y. Shi, X. Bian, N. Lv, S. Guo, Y. Wang, W. Zhao and W.-H. Zhu, Single-visible-light performed STORM imaging with activatable photoswitches, *Chem. Sci.*, 2025, **16**, 14270–14277.
19 X. J. Jiang, J. T. Lau, Q. Wang, D. K. Ng and P. C. Lo, pH– and thiol–responsive BODIPY–based photosensitizers for

targeted photodynamic therapy, *Chem. – Eur. J.*, 2016, **22**, 8273–8281.

20 A. M. Polgar and Z. M. Hudson, Thermally activated delayed fluorescence materials as organic photosensitizers, *Chem. Commun.*, 2021, **57**, 10675–10688.

21 M. Liu and C. Li, Recent advances in activatable organic photosensitizers for specific photodynamic therapy, *ChemPlusChem*, 2020, **85**, 948–957.

22 X. Li, S. Kolemen, J. Yoon and E. U. Akkaya, , Activatable photosensitizers: agents for selective photodynamic therapy, *Adv. Funct. Mater.*, 2017, **27**, 1604053.

23 Y. Wang, G. Wei, X. Zhang, F. Xu, X. Xiong and S. Zhou, A step-by-step multiple stimuli-responsive nanoplatform for enhancing combined chemo-photodynamic therapy, *Adv. Mater.*, 2017, **29**, 1605357.

24 E. Nestoros, A. Sharma, E. Kim, J. S. Kim and M. Vendrell, Smart molecular designs and applications of activatable organic photosensitizers, *Nat. Rev. Chem.*, 2025, **9**, 46–60.

25 Y. Xu, Y. Tang and Q. Li, Visible–and near–infrared light–driven molecular photoswitches for biological applications, *Adv. Funct. Mater.*, 2024, **22**, 2416359.

26 S. K. Bag, A. Pal, S. Jana and A. Thakur, Recent advances on diarylethene–based photoswitching materials: applications in bioimaging, controlled singlet oxygen generation for photodynamic therapy and catalysis, *Chem. – Asian J.*, 2024, **19**, 202400238.

27 M. J. Fuchter, On the promise of photopharmacology using photoswitches: a medicinal chemist's perspective, *J. Med. Chem.*, 2020, **63**, 11436–11447.

28 W. Piao, K. Hanaoka, T. Fujisawa, S. Takeuchi, T. Komatsu, T. Ueno, T. Terai, T. Tahara, T. Nagano and Y. Urano, Development of an azo-based photosensitizer activated under mild hypoxia for photodynamic therapy, *J. Am. Chem. Soc.*, 2017, **139**, 13713–13719.

29 J. Ji, X. Li, T. Wu and F. Feng, Spiropyran in nanoassemblies as a photosensitizer for photoswitchable ROS generation in living cells, *Chem. Sci.*, 2018, **9**, 5816–5821.

30 J. Wang, J. Wei, Y. Leng, Y. Dai, C. Xie, Z. Zhang, M. Zhu and X. Peng, Rational design of high-performance hemithioindigo-based photoswitchable AIE photosensitizer and enabling reversible control singlet oxygen generation, *Biosensors*, 2023, **13**, 324–335.

31 N. Sun, Y. Jin, H. Wang, B. Yu, R. Wang, H. Wu, W. Zhou and J. Jiang, Photoresponsive covalent organic frameworks with diarylethene switch for tunable singlet oxygen generation, *Chem. Mater.*, 2022, **34**, 1956–1964.

32 Z. Li, S. Chen, Y. Huang, H. Zhou, S. Yang, H. Zhang, M. Wang, H. Guo and J. Yin, Photoswitchable AIE photosensitizer for reversible control of singlet oxygen generation in specific bacterial discrimination and photocontrolled photodynamic killing of bacteria, *Chem. Eng. J.*, 2022, **450**, 138087.

33 S. K. Bag, B. Mondal, M. Karmakar, S. Das, A. Patra and A. Thakur, Controlled photooxidation via singlet oxygen generation by triplet harvesting in a heavy atom free pure organic dithienylethene–naphthalene diimide, *Chem. – Eur. J.*, 2024, **30**, 202401562.

34 T. Fukaminato, T. Sasaki, T. Kawai, N. Tamai and M. Irie, Digital photoswitching of fluorescence based on the photochromism of diarylethene derivatives at a single-molecule level, *J. Am. Chem. Soc.*, 2004, **126**, 14843–14849.

35 F. M. Raymo and M. Tomasulo, Electron and energy transfer modulation with photochromic switches, *Chem. Soc. Rev.*, 2005, **34**, 327–336.

36 J. Park, D. Feng, S. Yuan and H. C. Zhou, Photochromic metal-organic frameworks: reversible control of singlet oxygen generation, *Angew. Chem., Int. Ed.*, 2015, **52**, 11364–11368.

37 J. Ma, X. Cui, F. Wang, X. Wu, J. Zhao and X. Li, Photoswitching of the triplet excited state of diiodobodipy-dithienylethene triads and application in photo-controllable triplet-triplet annihilation upconversion, *J. Org. Chem.*, 2014, **79**, 10855–10866.

38 G. Liu, X. Xu, Y. Chen, X. Wu, H. Wu and Y. Liu, A highly efficient supramolecular photoswitch for singlet oxygen generation in water, *Chem. Commun.*, 2016, **52**, 7966–7969.

39 L. Hou, X. Zhang, T. C. Pijper, W. R. Browne and B. L. Feringa, Reversible photochemical control of singlet oxygen generation using diarylethene photochromic switches, *J. Am. Chem. Soc.*, 2014, **136**, 910–913.

40 T. M. Khang, P. Q. Nhien, T. T. K. Cuc, C. C. Weng, C. H. Wu, J. I. Wu, B. T. B. Hue, Y. K. Li and H. C. Lin, Dual and sequential locked/unlocked photochromic effects on FRET controlled singlet oxygen processes by contracted/extended forms of diarylethene–based [1] rotaxane nanoparticles, *Small*, 2023, **19**, 2205597.

41 U. Pischel, Chemical approaches to molecular logic elements for addition and subtraction, *Angew. Chem., Int. Ed.*, 2007, **46**, 4026–4040.

42 J. Andréasson and U. Pischel, Molecules with a sense of logic: a progress report, *Chem. Soc. Rev.*, 2015, **44**, 1053–1069.

43 J. Andréasson and U. Pischel, Smart molecules at work-mimicking advanced logic operations, *Chem. Soc. Rev.*, 2010, **39**, 174–188.

44 J. Andréasson and U. Pischel, Molecules for security measures: from keypad locks to advanced communication protocols, *Chem. Soc. Rev.*, 2018, **47**, 2266–2279.

45 S. Ozlem and E. U. Akkaya, Thinking outside the silicon box: molecular and logic as an additional layer of selectivity in singlet oxygen generation for photodynamic therapy, *J. Am. Chem. Soc.*, 2009, **131**, 48–49.

46 S. Erbas-Cakmak and E. U. Akkaya, Cascading of molecular logic gates for advanced functions: a self–reporting, activatable photosensitizer, *Angew. Chem., Int. Ed.*, 2013, **52**, 11364–11368.

47 S. Erbas-Cakmak, F. P. Cakmak, S. D. Topel, T. B. Uyar and E. U. Akkaya, Selective photosensitization through an AND logic response: optimization of the pH and glutathione response of activatable photosensitizers, *Chem. Commun.*, 2015, **51**, 12258–12261.

48 I. S. Turan, G. Gunaydin, S. Ayan and E. U. Akkaya, Molecular demultiplexer as a terminator automaton, *Nat. Commun.*, 2018, **9**, 805.
49 R. Campos-González, P. Vázquez-Domínguez, P. Remón, F. Nájera, D. Collado, E. Pérez-Inestrosa, F. Boscá, A. Ros and U. Pischel, Bis-borylated arylisoquinoline-derived dyes with a central aromatic core: towards efficient fluorescent singlet-oxygen photosensitizers, *Org. Chem. Front.*, 2022, **9**, 4250–4259.
50 G. Ur, J. Axthelm, P. Hoffmann, N. Taye, S. Glaeser, H. Goerls, S. L. Hopkins, W. Plass, U. Neugebauer and S. Bonnet, Co-registered molecular logic gate with a CO-releasing molecule triggered by light and peroxide, *J. Am. Chem. Soc.*, 2017, **139**, 4991–4994.
51 M. Herder, B. M. Schmidt, L. Grubert, M. Pätzel, J. Schwarz and S. Hecht, Improving the fatigue resistance of diarylethene switches, *J. Am. Chem. Soc.*, 2015, **137**, 2738–2747.
52 N. Menschutkin, Beiträge zur Kenntnis der Affinitätskoeffizienten der Alkylhaloide und der organischen Amine, *Z. Phys. Chem.*, 1890, **5**, 589–600.
53 S. Pal, Pyridine: a useful ligand in transition metal complexes, *Pyridine*, 2018, **57**, 57–74.
54 P. Corton, P. Novo, V. Lopez-Sobrado, M. D. Garcia, C. Peinador and E. Pazos, Solid-phase Zincke reaction for the synthesis of peptide-4,4′-bipyridinium conjugates, *Synthesis*, 2020, 537–543.
55 N. Sun, C. Wang, H. Wang, X. Gao and J. Jiang, Photonic switching porous organic polymers toward reversible control of heterogeneous photocatalysis, *ACS Appl. Mater. Interfaces*, 2020, **12**, 56491–56498.
56 C. Hatchard and C. A. Parker, A new sensitive chemical actinometer-II. Potassium ferrioxalate as a standard chemical actinometer, *Proc. R. Soc. London, Ser. A*, 1956, **235**, 518–536.
57 H. Kuhn, S. Braslavsky and R. Schmidt, Chemical actinometry, *Pure Appl. Chem.*, 1989, **61**, 187–210.
58 T. Sumi, Y. Takagi, A. Yagi, M. Morimoto and M. Irie, Photoirradiation wavelength dependence of cycloreversion quantum yields of diarylethenes, *Chem. Commun.*, 2014, **50**, 3928–3930.
59 M. Roseau, V. De Waele, X. Trivelli, F. X. Cantrelle, M. Penhoat and L. Chausset-Boissarie, Azobenzene: a visible–light chemical actinometer for the characterization of fluidic photosystems, *Helv. Chim. Acta*, 2021, **104**, 2100071.
60 R. W. Redmond and J. N. Gamlin, A compilation of singlet oxygen yields from biologically relevant molecules, *Photochem. Photobiol.*, 1999, **70**, 391–475.
61 J. Chen-Wu, D. B. Guzmán-Ríos, P. Remón, J. A. González-Delgado, A. J. Martínez-Martínez, F. Nájera, J. F. Arteaga and U. Pischel, Photofunctional scope of fluorescent dithienylethene conjugates with aza–heteroaromatic cations, *Adv. Mater.*, 2023, **35**, 2300536.
62 It can not be excluded that also PeT from the ring-closed DTE core to the excited singlet-state anthracene dicarboximide contributes to the observed quenching of fluorescence and $^1O_2$ formation in **1c**; see SI.